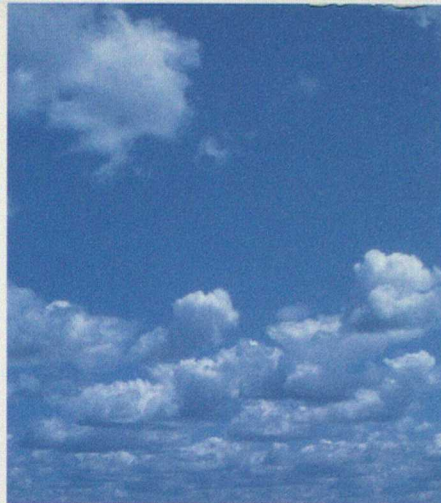


Hadley Centre

for Climate Prediction and Research



Representation of the Radiative Effect of Convective Anvils

by

Julie Gregory

HCTN 7

April 1999

Hadley Centre Technical Note



The Met.Office

HADLEY CENTRE TECHNICAL NOTE NO. 7

REPRESENTATION OF THE RADIATIVE EFFECT OF
CONVECTIVE ANVILS

by

Julie Gregory

April 1999

Hadley Centre for Climate Prediction and Research
Meteorological Office
London Road
Bracknell
Berkshire RG12 2SY

NOTE: This paper has not been published. Permission to quote from it should be obtained from the Director of the Hadley Centre.

© Crown Copyright 1999

Representation of the Radiative Effect of Convective Anvils

Julie Gregory

23rd March 1999

1 Abstract

A parametrization of the radiative effects of convective anvils is presented. A vertical profile is prescribed for convective cloud amount, and cloud water contents are adjusted to be close to cloud resolving model results. Satellite observations are used to determine parameters required by the scheme. Off-line single column radiation calculations are performed to show the direct impacts of the scheme and illustrate the change in the vertical profile of radiative heating rates. These show that the new anvil profile of convective cloud provides a broad heating in the mid-upper troposphere. Results of the scheme in the atmosphere only version of the latest Hadley Centre climate model are presented. Top of atmosphere radiative biases and systematic errors in cloud amount and type are reduced. The scheme increases longwave and shortwave cloud forcing in the tropics and causes a warming of the upper tropical troposphere. Possible feedbacks and limitations of the scheme are discussed.

2 Introduction

Radiative forcing from convective anvils plays a dominant role in determining the vertical profile of radiative heating in the tropics and so modulating the general circulation. Anvil clouds from mesoscale convective systems (MCSs) are optically thick, spatially extensive and can persist for days. These qualities mean that anvils have a profound influence on the components of the top of atmosphere (TOA) radiative fluxes in the tropics. This can be seen in satellite observations eg. the Earth Radiation Budget Experiment (ERBE) (Barkstrom, 1984). Field studies (eg. the Tropical Ocean Global Atmosphere Coupled Ocean Atmosphere Response Experiment (TOGA COARE), Moncrieff *et al.* (1997)) show that these clouds are associated with deep convection and can develop their own mesoscale circulation.

Convection is almost always subgrid scale, so has to be parametrized. However, the mesoscale circulation associated with MCS anvils can be resolved for some finer grids. The wide range of time scales associated with convection from about an hour for shallow convection to days for MCSs can also give rise to problems. Many General Circulation

Models (GCMs) including the Met. Office Unified Model (UM) use a quasi-equilibrium assumption so do not explicitly represent the life-cycle of different systems.

The problems associated with parametrizing convective cloud and anvils give rise to a wide range of treatments in modern GCMs. Methods for calculating convective cloud fraction can broadly be divided into two main types. First we shall consider the diagnostic approach. Cloud amount is related to large-scale relative humidity (RH) or, in some schemes, the strength of convection. In the former, cloud is diagnosed when the gridscale RH reaches a critical value. Convective processes input into these schemes through their vertical transport of moisture which then changes RH when detrainment, entrainment and precipitation occur. The latter type of diagnostic scheme relates the convective cloud amount to a measure of the convective activity. For example Slingo (1987) uses an empirical relation between the convective precipitation and cloud fraction. Schemes can further be divided into continuous, where the cloud fraction can be anything between 0 and 1, and discrete, where only fractions of zero and one are allowed. One version of the UCLA/GLA GCM uses the depth of convection to implement a discrete scheme: Randall *et al.* (1989) assume convective cloud amount is negligible except when it penetrates 400 hPa, when it is assumed that an anvil covers the entire gridbox from this level to the cloud top. The other main type of convective cloud parametrization is the prognostic approach. Convection is then one physical process which contributes to a prognostic cloud amount and water content eg. Tiedtke (1993). This type is more computationally expensive than the diagnostic method but benefits include the consistent treatment of layer and convective clouds.

In a recent study Zender and Kiehl (1997) (from hereon ZK97) look at the sensitivity of the NCAR Community Climate Model (CCM) to a prognostic anvil parametrization. A number of observed microphysical characteristics of anvils are incorporated including enhanced ice content in the anvil, the observed vertical distribution of condensate, and the link between cloud base mass flux and anvil growth rate. An anvil cloud fraction of 1 is assumed which, as ZK97 notes, is probably an overestimation. In the present study a diagnostic scheme is implemented through modification to the cloud amount with a simpler microphysical treatment: the vertical variation in radiative heating rates is captured through the cloud fraction profile rather than the condensate profile as in ZK97.

Only the radiative effects of convective anvils are considered here. Anvil clouds in MCSs develop a circulation secondary to that in the convective tower. A couplet of ascent within the cloud and a mesoscale downdraught below provide extra heating and cooling in the column. The mesoscale updraught also provides a further moisture source in addition to the input from the convective tower. No attempt has been made here to represent these thermodynamic and microphysical impacts of anvils, although work is underway at the Met. Office to do this (Gray, personal communication).

Section 2 describes the control GCM used in this study; section 3 details its systematic errors and shows why the anvil scheme is required. Section 4 describes the nature of the parametrization and details how various parameters required by the scheme were chosen. In section 5 some idealised single column radiative heating rates and fluxes are shown and described. Results of full GCM integrations are given in section 6 and a

summary and conclusions are given in section 7.

3 The Model

The GCM experiments described in this paper employ a version of the UM. In particular, they are based on a version of the Hadley Centre climate model, HadAM3 (Hadley Centre Atmospheric Model version 3) with some enhancements. HadAM3 and its climatology are described in Pope *et al.* (1999). The differences from hadAM3 are as follows:

- an ice microphysics scheme (described in Wilson and Ballard (1999))
- a change to the layer cloud amount using a vertical gradient cloud area scheme where each layer is split into three and the cloud volume in each is dependent on the gradient of thermodynamic variables between model levels (Cusack, personal communication)
- a revised boundary layer scheme which includes non-local mixing and a parametrization of entrainment (Martin *et al.*, 1998)
- 38 levels in the vertical (as opposed to 19 in HadAM3): 8 of the extra levels are in the boundary layer (Martin *et al.*, 1998)
- a parametrization of sub-grid variability of total water content is included (Cusack *et al.*, 1999)
- in the radiation scheme (Edwards and Slingo, 1996) a parametrization of non-spherical ice is used as well as a pre-industrial ozone climatology derived from AMIP II ozone (Stratton *et al.*, 1998) and updated spectral files
- the orography around Antarctica has been updated

Other smaller differences include a change in the cloud droplet number concentration, a revision to run-off basins in the land-surface scheme, some land albedo changes and a different maximum effective radius for convective clouds.

The mass flux convection scheme in the UM (Gregory and Rowntree, 1990) uses an ensemble of entraining and detraining plumes to determine the transports of properties within updraughts and downdraughts in the grid-column. It detrains cloudy air and water throughout the convecting layer, increasing the relative humidity in the column. The large-scale cloud scheme can then produce an appropriate amount of layer cloud. This is not good enough to represent the radiative effects of an anvil because it produces clouds spread over the entire climate gridbox which are frequently too optically and geometrically thin. Also errors in the detraining rate profile lead to errors in the cloud amount and water content. In addition to the response of the large-scale cloud scheme to convection, a convective cloud fraction is also incorporated. It might therefore be suggested that a double counting of convective cloud exists in the model. It is argued here that the diagnostic layer cloud scheme cannot adequately represent anvils. Firstly,

as mentioned above, they are too optically thin. Secondly they do not have the correct vertical structure, and horizontal variation of optical depth. These thin cirrus that persist after the convection scheme has switched off can be thought of as the detrainment from the anvils themselves. These clouds are optically thin debris from deep convective events. The anvil scheme described in this paper is intended to bridge the gap between the thin cirrus of convective origin and the deep convective towers.

The control UM calculates convective cloud fraction diagnostically through an empirical relation to the total water flux. In a similar manner to Slingo (1987), convective cloud fraction is related to the logarithm of a water flux. The formula used at present is as follows:

$$CCA = a + b \cdot \log(TCW)$$

where TCW is a total cloud water flux and a and b are constants. This gives a variation of cloud fraction with rain rate approximated in figure 1.

In the control UM scheme cloud fraction is not allowed to vary with height within a gridbox. It is simply applied as a constant value between the diagnosed ensemble cloud base and top. Typical values produced by the scheme are of the order a third. This is an overestimation of cloud amount produced by deep convective towers alone, but an underestimate of a typical anvil cloud fraction. Figure 2 shows a zonal mean cross-section of convective cloud amount for the season June-July-August (JJA) from the UM.

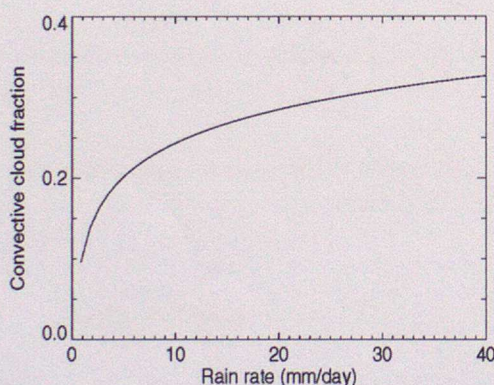


Figure 1: Variation of cloud fraction with rain rate

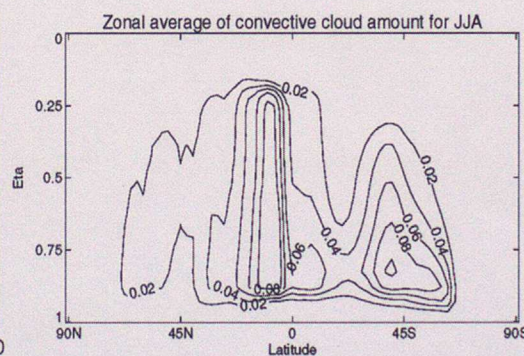


Figure 2: Zonal mean convective cloud amount

Convective cloud water in the control model is calculated in the parcel ascent of the mass flux scheme. When the cloud water exceeds a certain threshold (set to $1g/kg$) and the cloud meets certain other criteria (such as a critical depth, or glaciation) excess water above the threshold is removed from the layer as precipitation. The radiation scheme sees the cloud water path (including precipitation) from the convection scheme and divides it into layers of equal condensate mass mixing ratio (mmr).

4 Systematic errors and deficiencies in the model

To achieve a realistic vertical profile of radiative heating rates in the tropics we must provide a good simulation of both the cloud amount and condensate. These determine the optical thickness of the cloud and its properties in both the longwave and shortwave parts of the spectrum. In the tropics, convective cloud is predominantly responsible for determining these radiative effects.

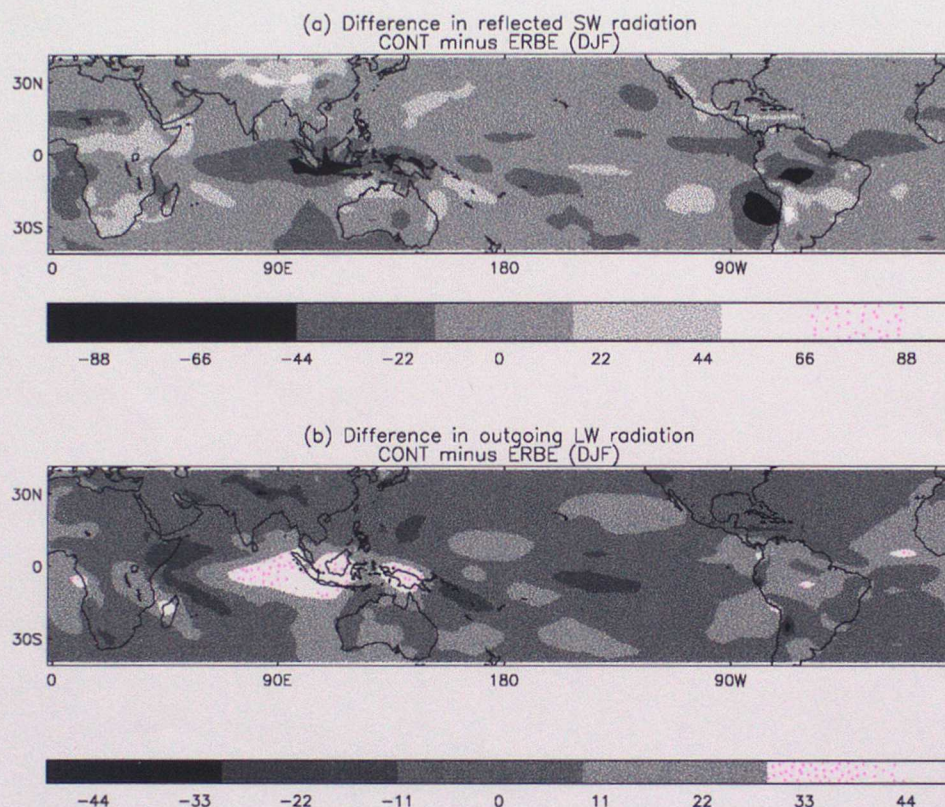


Figure 3: Difference in reflected shortwave radiation and outgoing longwave radiation (W/m^2) for a five year average of winter (December, January and February): control minus ERBE.

The control has too much outgoing longwave radiation (OLR) and too little reflected shortwave radiation (RSW) with respect to ERBE: the tropical cloud forcings are too low. Figure 3 (a) shows that the control UM has too little RSW in the ITCZ particularly in the western Pacific and the Indian Ocean. Figure 3 (b) shows that the control simulation has too much OLR in the western Pacific warm pool, extending into the Indian Ocean.

A tool used to give further information on both cloud shape and water contents is ISCCP data (Rossow and Schiffer, 1991). This gives frequencies of occurrence of clouds for three ranges of cloud optical thickness; (thin: < 3 , intermediate: $3 - 25$ and thick:

> 25) and three ranges of cloud top pressure; (high: $< 440mb$, medium: $440 - 680mb$, low: $> 680mb$). Figures 4 and 5 show that the model has too much optically thick cloud and not enough cloud of intermediate optical depth. Together, this means the model has too little convective cloud, but excessive water paths. Also, the control convective cloud fractions that are constant with height do not provide a very realistic profile of radiative heating. This affects the model's circulation. The anvil scheme is expected to address these errors.

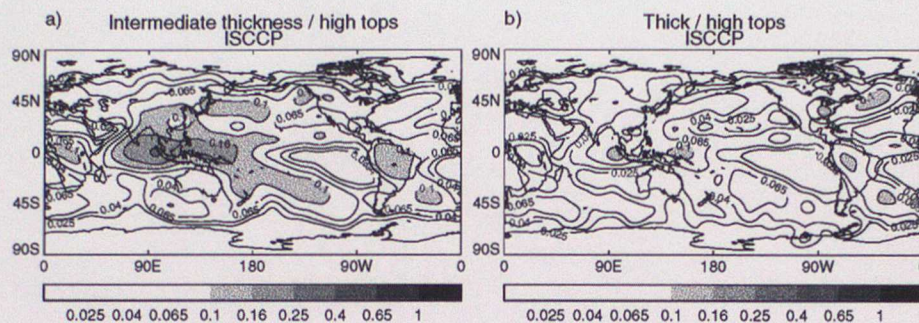


Figure 4: Amounts of medium and high optical thickness clouds with high cloud tops in July 1988: ISCCP

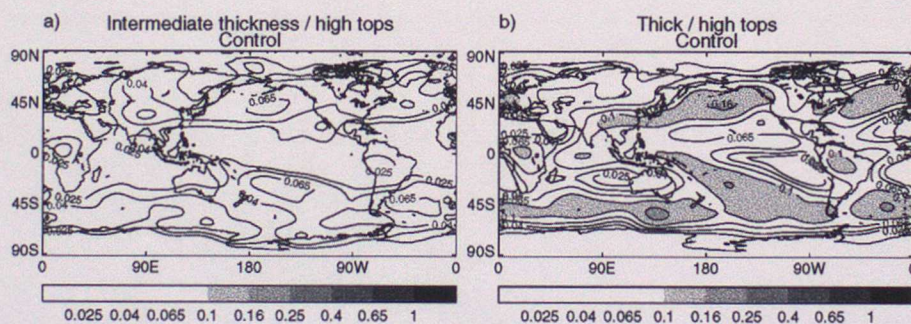


Figure 5: Amounts of medium and high optical thickness clouds with high cloud tops in July 1988: CONT

More realistic convective cloud water contents are also introduced. The control model includes convective precipitation in the water path seen by the radiation scheme. This is incorrect to first order: it is more realistic to neglect precipitation altogether than to assume it is all highly reflective cloud droplets or ice particles.

Figure 6 shows convective cloud water profiles from a case study of the GEWEX Cloud System Study (GCSS) working group 4 (Moncrieff *et al.*, 1997). Several Cloud Resolving Models (CRMs) and Single Column Models (SCMs) are forced with observational data from TOGA COARE in the western Pacific. It is clear that the SCM version

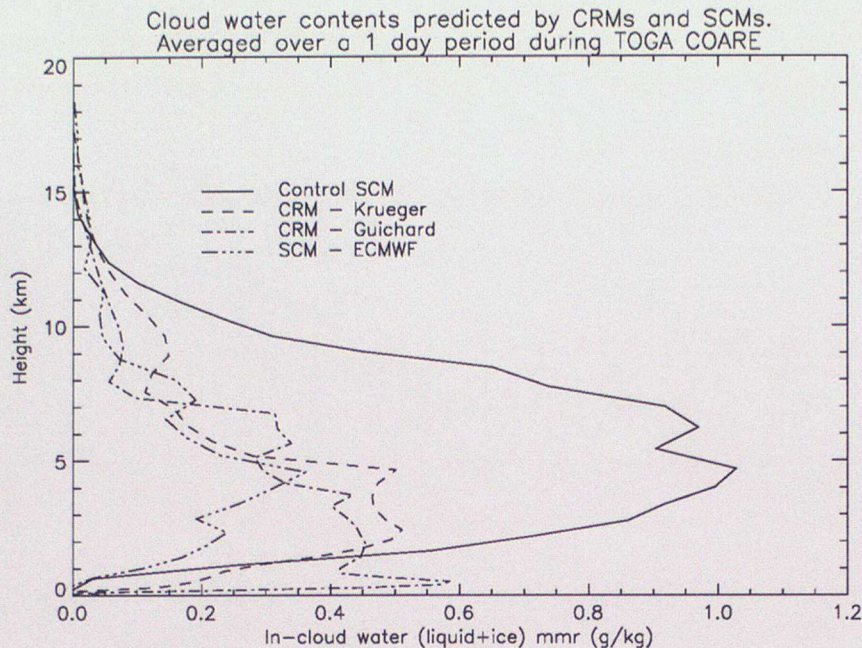


Figure 6: Cloud water profiles for CRMs involved in GCSS working group 4 case 2

of the control UM has excessive water contents throughout the depth of the cloud.

The aim of this work is to provide a better radiative forcing of the model in the tropics and an improved vertical profile of heating rates (which might also improve the model's circulation) for the new Hadley Centre coupled model, HADCM4. It is hoped that a less empirical scheme can be developed in the future. However, the anvil scheme is desirable in the interim because it directly addresses known model systematic errors and it is more realistic than the control convective cloud parametrization. In particular it produces top of atmosphere fluxes of long and shortwave radiation in better agreement with observations (see section 6).

5 Description of the parametrization

The lack of vertical variation of cloud amount in the control scheme is a severe shortcoming that constrains the model. This constraint is relaxed here to address the errors in radiative fluxes in the tropics and to improve the vertical profile of radiative heating rates. The new scheme takes the cloud amount predicted by the control method and calculates a new cloud amount that varies with height. Some basic observations of anvils are incorporated into the scheme. Firstly, that they are associated with deep convection rather than shallow, and secondly that they are ice clouds that tend to have their bases at the freezing level.

The Slingo (1987) scheme uses a number of criteria to modify the cloud fraction which would not normally vary with height. When convection is diagnosed as deep then

the cloud fraction takes a quarter of the original fraction, C . A high cloud amount is also added with fraction $2(C-0.3)$ and a low cloud with three-quarters of C is included to represent shallow convection occurring elsewhere in the gridbox. Note that the high and low clouds each occupy one model layer. This has implications for the vertical profile of radiative heating rates, as discussed in Slingo and Slingo (1988). A cloud in a single layer cannot resolve the cloud top cooling and cloud base warming dipole. Instead the two effects get added together (usually producing a net warming). This may impact upon the circulation of the parent model.

The present scheme modifies convective cloud amount in the presence of deep convection. The cloud fraction is increased linearly with model level from the freezing level to the cloud top to represent the anvil, and decreased to a constant value below the freezing level to represent the convective tower. This revised convective cloud fraction is used in the radiation scheme. Deep clouds are defined as those having their bases in the boundary layer and their tops above the freezing level. If convection is not diagnosed as deep then no change is made to the cloud fraction. An overall depth criterion for deep clouds was considered where only clouds greater than (say) 500 hPa in depth would have an anvil. However in trials of the anvil scheme in the coupled ocean-atmosphere version of the UM the tropical SSTs improved but a Southern Ocean warm bias worsened. Although there are rarely clouds deep enough to get anvils in the Southern Ocean, the reduction in convective cloud water meant more SW radiation reached the sea surface and heated it. To counteract this anvils were allowed to occur at high latitudes by relaxing the criterion that clouds had to be 500 hPa deep. Convection is less vigorous in the Southern Ocean than in the tropics so the convective cloud fractions are smaller. This leads to smaller anvils. In Ludlam (1980) there is evidence of smaller anvils occurring at high latitudes eg. over Sweden. The resultant model had the desired effect of brightening the Southern Ocean and taking the warm ocean bias back to the level it was in the control. It is also desirable to remove the depth criterion because there are then less parameters to be chosen in the scheme.

Convective cloud water is reduced in two ways (i) by excluding water precipitating from a layer from the water path and (ii) by further reducing the remaining cloud water which is still high compared to observations. (i) is justified to first order because rain drops are much less radiatively active than cloud droplets which are significantly smaller. An initial attempt at (ii) was achieved by increasing the precipitation efficiency of the convection. The threshold above which water was rained out of a layer was reduced from 1g/kg to 0.2g/kg. This improved agreement in optical depths with ISCCP data, but had other unfortunate side-effects. It changed the nature of convection itself: the parametrization was no longer purely radiative. The increased efficiency of precipitation caused a drying of the tropical troposphere. This made certain systematic errors in the model worse. For example figures 7 and 8 show how the column integrated water content in the tropics, which was already too low, is decreased further when the precipitation efficiency is increased. Also, there is no real justification to use precipitation efficiency as a means of reducing convective cloud water. For these reasons the precipitation threshold was put back to 1g/kg.

To counter this, another way of reducing the convective cloud water was sought. An

'updraught factor' was introduced to reduce the convective cloud water without directly changing convection. The updraught generally takes up only a small proportion of the cloud and yet this is what the convective cloud water calculated by the mass flux convection scheme's parcel ascent most closely represents. One would naively assume that the updraught factor should be set to 0.2 to counteract putting the precipitation threshold back up to 1 g/kg. However, increasing the threshold has multiple repercussions:

- it increases the amount of water left in a layer
- it reduces the frequency of precipitation because the cloud water in the layer must be greater than the threshold before it rains
- it indirectly affects the frequency of convection so there are fewer periods of no convection
- through increasing the amount of water left in a layer it increases the amount detrained out at each level and consequently the layer cloud amount.

All of the above changes act to increase the time average convective cloud forcing. To counteract all this, a suitable value of updraught factor was found to be 0.12.

Figure 9 shows the average in-cloud water contents obtained from the SCM version of the UM. The profiles are mean values for a day in the December 1992 TOGA COARE intensive observation period (IOP). It is clear that the cloud water content is dramatically reduced when precipitation is not included in it. This is not just a matter

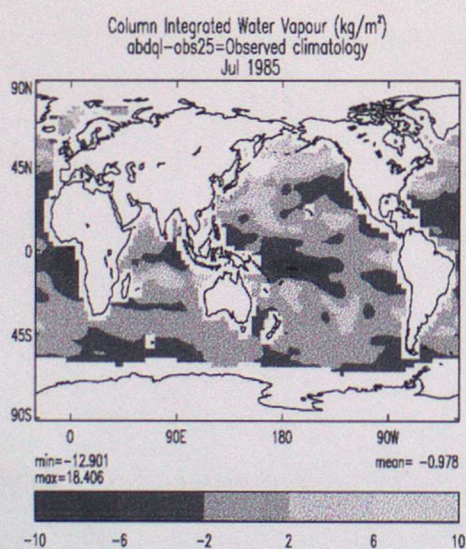


Figure 7: Experiment with precipitation threshold of 1g/kg

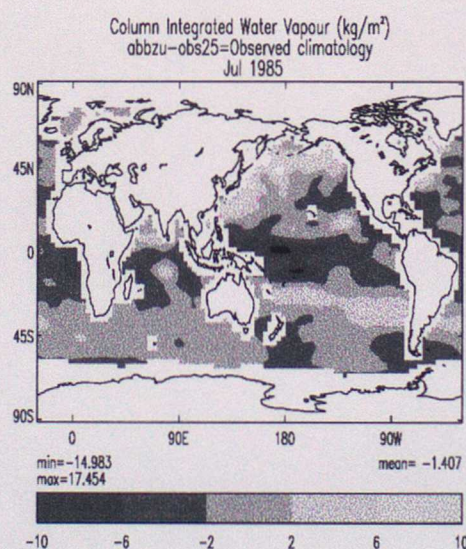


Figure 8: Experiment with precipitation threshold of 0.2g/kg

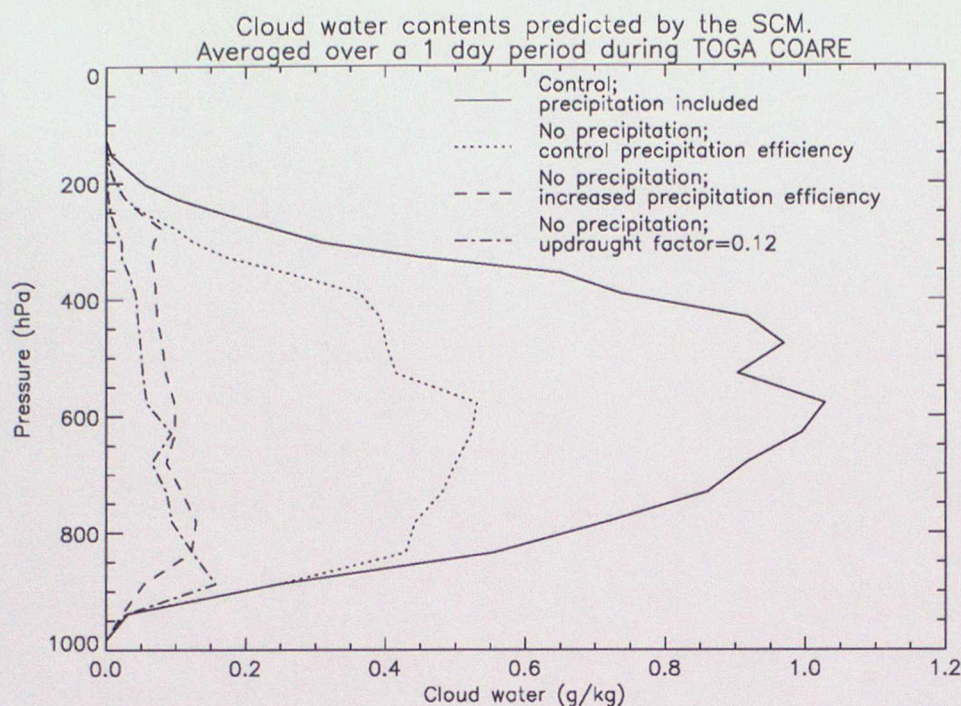


Figure 9: Cloud water profiles for varying assumptions in the SCM version of the UM.

of definition, but what the radiation scheme uses to calculate fluxes and heating rates. The cloud water is further reduced to 0.1g/kg when the precipitation efficiency is increased. It is also shown that this value can be achieved by instead using an updraught factor of 0.12. Comparison with figure 6 shows that the reduced water contents are in better agreement with CRM results.

This formulation requires the specification of factors by which the original cloud fraction is multiplied to determine the shape of the cloud (figure 10). Satellite data can be used to constrain this choice. The anvil and tower factors that give the best agreement with measurements from ERBE can be chosen by making the assumption that anvil clouds dominate radiative balance in the tropics. A larger anvil factor traps more LW radiation and reflects more SW. The values arrived at through this process were an anvil factor of 3 and a tower factor of 0.25.

The anvil scheme addresses the excess amount of thick cloud by removing some of the cloud water. It also increases the amount of cloud with intermediate optical thickness (which the control model lacks) using the anvil shape. Results are shown in section 7.

6 Off-line single column radiation experiments

The GCM radiation code (Edwards and Slingo, 1996) is here used to calculate radiative heating rates and fluxes for a single column of the atmosphere (representative of a column of GCM grid boxes) with specified profiles of temperature, humidity and cloud variables.

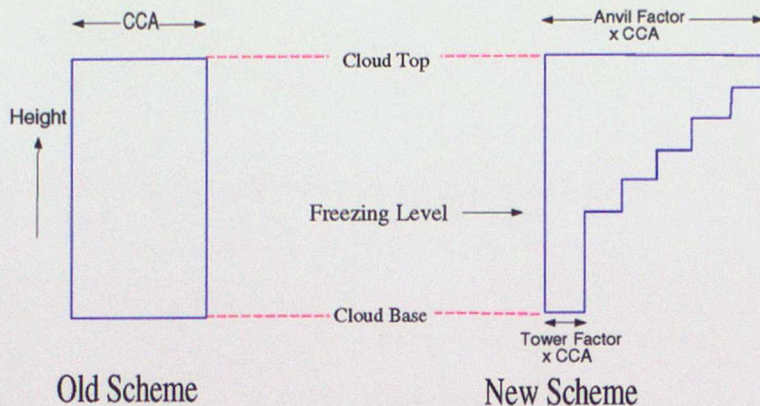


Figure 10: Schematic diagram of anvil scheme

These experiments have the advantage of showing the direct effects of the changes in cloud shape and water content without the complication of feedbacks which are present in a GCM. The impact of each change can also be assessed separately.

Temperature and humidity profiles are taken from the standard McClatchey atmosphere dataset for the tropics (McClatchey *et al.*, 1972). Cloud fractions and cloud ice and water content must also be specified. Many different calculations were performed, exploring the sensitivity to cloud amount, cloud shape, cloud water path and solar zenith angle. A clear sky calculation served as a means of deriving the longwave and shortwave cloud forcing heating rates. In all the cloudy experiments, a deep cloud with its base around 900 hPa and top near 200 hPa was used. Cloud water mixing ratios of 0.1, 0.2, 0.5 and 1 g/kg were tried. This represents the full range of mixing ratios used by the GCM in the experiment and control. For each case an anvil-shaped cloud was compared to a uniform cloud fraction with height (as in figure 5). The cloud fraction at cloud top was kept the same for most comparisons between the control and anvil. Zenith angles of 0, 30 and 60 degrees were used: the results were qualitatively the same. The discussion will therefore be limited to experiments with a zenith angle of 30 degrees.

Figure 11 shows how the outgoing fluxes of longwave and shortwave radiation vary with cloud top fraction for uniform clouds and for clouds with an anvil. The reflected solar flux increases with cloud fraction, and the uniform cloud is brighter than that with the anvil which tapers towards the freezing level. The difference between the two curves narrows as water path increases (figure 11(c)), and the anvil portion of the cloud approaches saturation in the shortwave. Since longwave radiation quickly becomes saturated for only relatively small water paths, the outgoing longwave radiation is almost identical for the anvil and control: in the infra-red they appear the same from above. This behaviour means that an increase in water path has very little effect in the longwave (fig 11(d)).

Figure 12 shows the longwave and shortwave cloud forcing of heating rate (all-sky minus clear-sky values) for a uniform cloud and for one with an anvil. Again, both

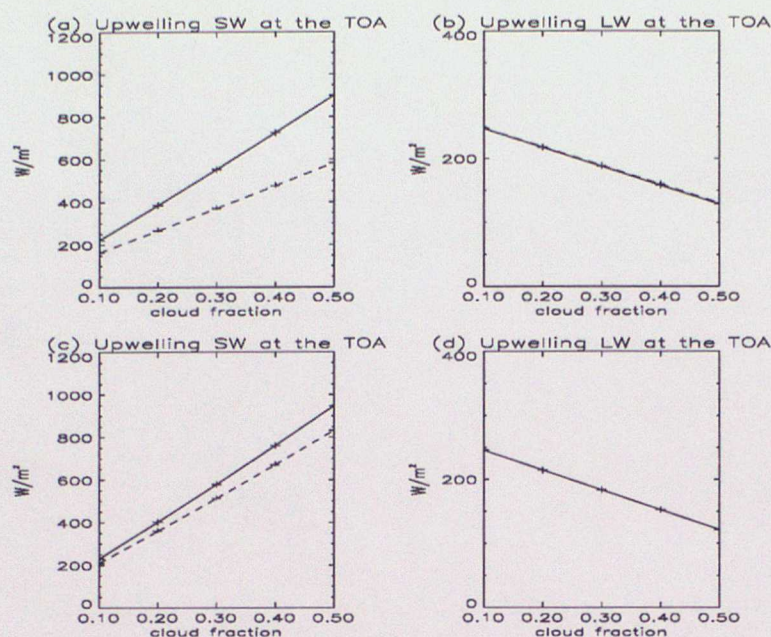


Figure 11: Variation of TOA fluxes with cloud amount for a uniform cloud (solid) and one with an anvil (dashed). The top two plots are for cloud water contents of 0.1g/kg; the bottom two for 1g/kg

clouds have the same fraction as seen from above, and the same in-cloud water mmr.

The cloud top cooling in the longwave is very similar for both clouds because they appear the same from above. Further down the cloud, however, the anvil has more of a warming effect. This is due to warming through absorption of longwave radiation in the region of the anvil base. Even further down, between the freezing level and the surface, the anvil cloud has less of a warming effect than the control. This is because the lower cloud fraction in the region of the 'tower' allows more clear-sky cooling. There are two competing effects here: (i) the presence of the anvil causing cloud base warming and (ii) the lower cloud fraction of the anvil cloud giving rise to enhanced longwave cooling. The dominating effect changes where the two curves cross.

In the shortwave the cloud top absorption is initially the same for both clouds. However, the heating in the anvil falls away more quickly than in the control because the cloud tapers towards the freezing level. Although the reduced cloud amount in the anvil reduces the heating from absorption of shortwave, it allows a larger flux to reach the lower part of the cloud. This gives rise to two effects. Firstly, there will be a greater absorption per unit area of cloud in the anvil tower because of the larger radiative flux. Secondly the anvil tower will reflect less radiation because of the smaller cloud fraction thus reducing the cooling effect of cloud.

Figure 13 shows the longwave and shortwave cloud forcing of heating rates for four different convective clouds. The intention is to show the effect of each of the individual changes introduced to the GCM. This time the cloud fractions as seen from above are

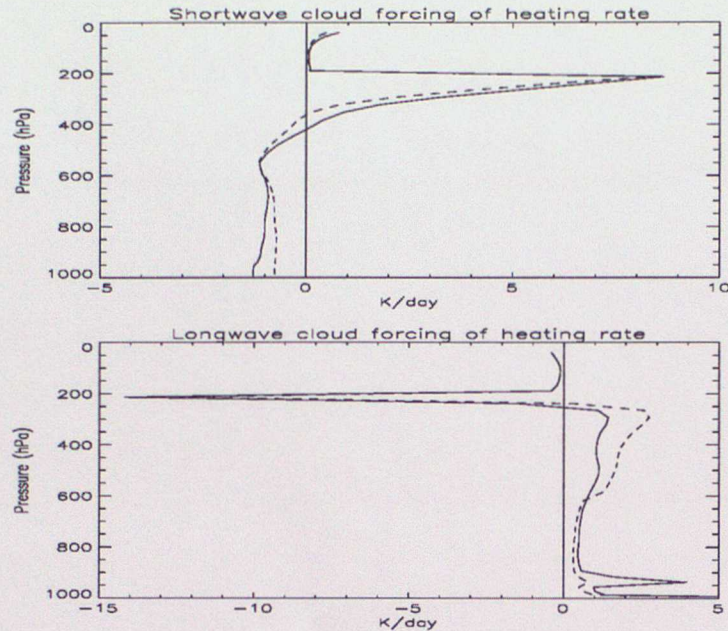


Figure 12: Longwave and shortwave heating rates minus clear sky values for control (solid) and anvil (dashed) for a cloud fraction of 0.6 as seen from above and a cloud water mmr of 0.1g/kg. Solar zenith angle is 30 degrees.

not the same. Instead they are in the same ratio as they are in the GCM for the control and anvil experiments i.e. the anvil cloud top fraction is twice that of the control, tapering to the freezing level where it remains at a quarter of the control cloud amount down to the cloud base.

The plot of shortwave cloud forcing of heating rate shows that changing the shape of the cloud (as in fig 10) increases the heating near cloud top (above 260 hPa in this case). Below, the effect of the new cloud shape is to cool the column slightly. When the cloud water of the control cloud is reduced by a factor of ten the shortwave heating at cloud top is dramatically reduced. However, there is less attenuation of the shortwave flux because of the lower cloud water contents. Absorption of this extra radiation results in a warming relative to the control below 250 hPa. The resultant effect of the reduced cloud water and the anvil shows a warming relative to the control between 450 and 250 hPa, a cooling above and little change below.

In the longwave the anvil has a much greater cloud top cooling than the control. Below, however, there is a combination of reduced cooling (due to the higher cloud fraction) and cloud base warming (due to the anvil itself). These effects result in a warming relative to the control between 240hPa and just above the cloud base. The much broader base of the control cloud shows a peak from absorption (around 900 hPa). The reduction in water content has little effect on the profile of longwave heating rates in contrast to the effect in the shortwave. This is due to the saturation effect in the longwave. Differences can be seen in the cloud top cooling and in the slightly reduced

cooling very close to the cloud top, before the water path reaches saturation in the longwave. So the combined effect of the anvil and reduced water content is very similar to that of the anvil alone: an increase in cooling at cloud top, and an increase in warming below.

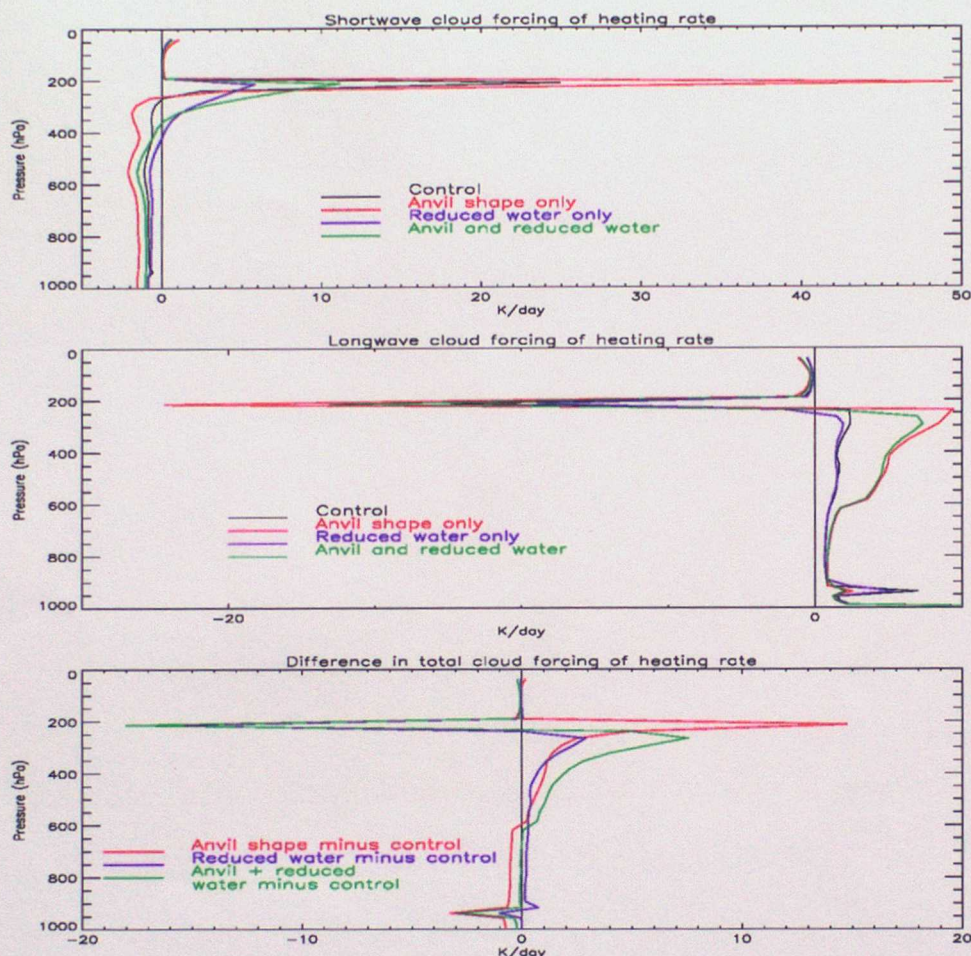


Figure 13: Longwave, shortwave and total cloud forcing of heating rates showing the impact of each of the aspects of the anvil scheme.

Figure 13(c) shows the difference in total cloud radiative forcing heating rate between each of the cloud types and the control. The anvil with reduced water curve shows the forcing given to the GCM: an enhanced cooling at cloud top and a deep warming below, mainly above the freezing level. The net warming in the mid-upper troposphere results from contributions from both the longwave and shortwave parts of the spectrum. This difference in the vertical profile of radiative heating rates will help address the cold bias present in the GCM. These offline radiation tests have also shown it is possible to change the anvil properties, within observed limits, to achieve top of atmosphere radiative balance (see figure 11) in the absence of feedbacks: both the shape of the anvil

and the water path can be varied so that the best agreement with ERBE TOA cloud forcing in the tropics can be achieved. This can be justified in the tropics by assuming that convective clouds are the dominant forcing for radiation. When the scheme is put into a GCM it is possible that feedbacks will modify the impact of the anvil. This is discussed further in section 7.

7 GCM results

Two five year integrations of the GCM were carried out. The control ('CONT') contained a cloud fraction uniform with height and water contents of typically more than 1g/kg. The experiment ('ANVIL') contained the anvil scheme applied to all clouds with their base in the boundary layer and their top above the freezing level. Cloud water contents were reduced using an updraught factor of 0.12 and by exclusion of precipitation from the water path.

The direct effects of the anvil scheme are as expected. Placing more convective cloud in the tropics increases both the longwave and shortwave cloud forcing there. Figure 14 shows the difference between ANVIL and ERBE in outgoing SW and LW radiation. A comparison of figures 14(a) and 3(a) shows that ANVIL has increased RSW in the ITCZ, particularly in the western Pacific warm pool and Indian ocean, improving agreement with ERBE. However there is now too much RSW in some regions, notably east of Papua New Guinea and in the western Indian ocean. Comparison of figure 14(b) with figure 3(b) shows that the anvil scheme has reduced the OLR right across the ITCZ, particularly the western Pacific warm pool and Indian ocean. This improves agreement with ERBE in the warm pool but there is now too little OLR in some areas e.g. the western Indian and mid-Pacific oceans.

A direct effect of the the anvil scheme is to increase the amount of cloud with high tops and intermediate optical depths. The zonal mean convective cloud amount predicted in ANVIL is shown in figure 15 (cf figure 2). Figure 16 shows the frequencies of occurrence of clouds with high tops and high and medium optical thickness. A comparison of this with figures 4 and 5 shows that the amount of intermediate thickness cloud is increased in the tropics along the ITCZ and in the west Pacific in ANVIL relative to CONT. This constitutes a significant improvement, although this type of cloud is still underestimated with respect to ISCCP. The excessive amounts of thick clouds with high tops present in the tropics in CONT are reduced in ANVIL.

The anvil scheme gives rise to a widespread and beneficial warming of the tropical troposphere, particularly at upper levels. This effect is shown in figure 17. This also shows the cold bias present in CONT with respect to ECMWF reanalyses. The cooling at the tropopause and in the stratosphere in ANVIL also reduces a systematic error present in CONT. The change in radiative heating rates shown in section 6 shows that the anvil causes a warming in the mid-upper troposphere as seen here. However the GCM results contain responses and feedbacks from other physics schemes and the dynamics of the UM. One possible example of this is the stabilization of the troposphere caused by the radiative heating high up. This in turn could curb convective intensity and hence

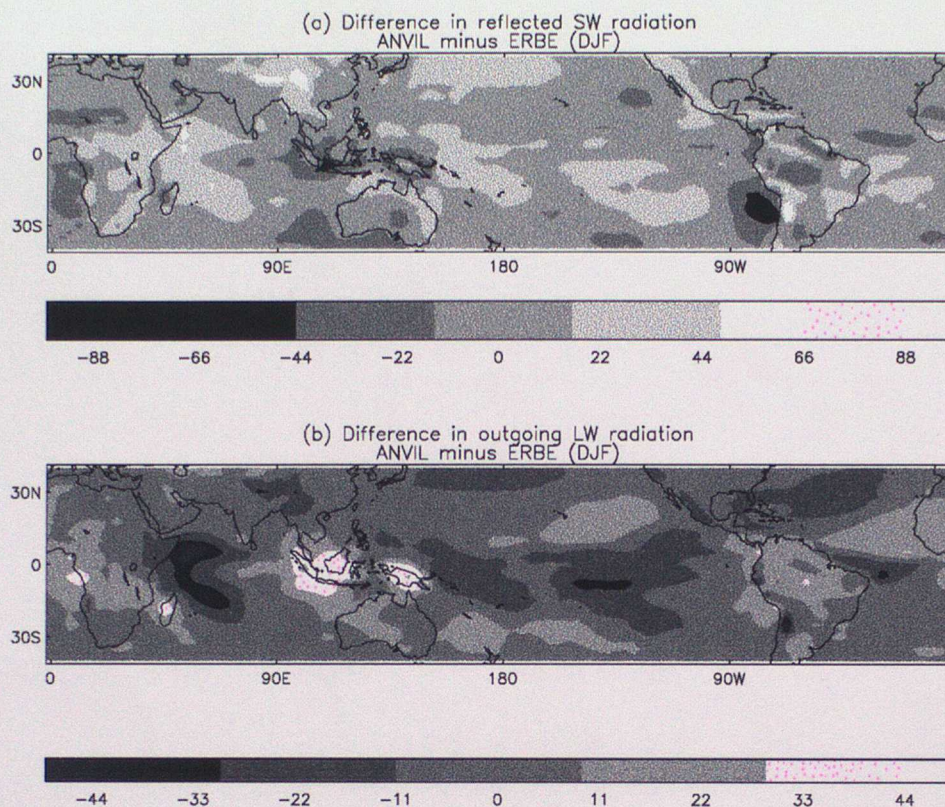


Figure 14: Difference in reflected shortwave radiation and outgoing longwave radiation (W/m^2) for a five year average of winter (December, January and February): ANVIL minus ERBE.

heating. In this case the radiative change dominates the convective effects so that the heating appears in the seasonal average.

Changes in circulation may also arise from changes in tropospheric temperature. This is another source of feedbacks. ANVIL has a narrower band of precipitation across the Pacific and a more continuous maximum in the SPCZ (not shown). The divergence at 250 hPa and convergence at 850 hPa in the SPCZ are stronger in ANVIL and more continuous than those in CONT. This change in circulation is consistent with the change in precipitation in this region.

8 Conclusions and Future Work

A scheme to represent the radiative effects of convective anvils has been developed and tested. This scheme diagnoses a vertical distribution of convective cloud amount to give a realistic variation of cloud fraction with height. It also prescribes realistic cloud water contents. When implemented in the Hadley Centre climate model, the new scheme gives

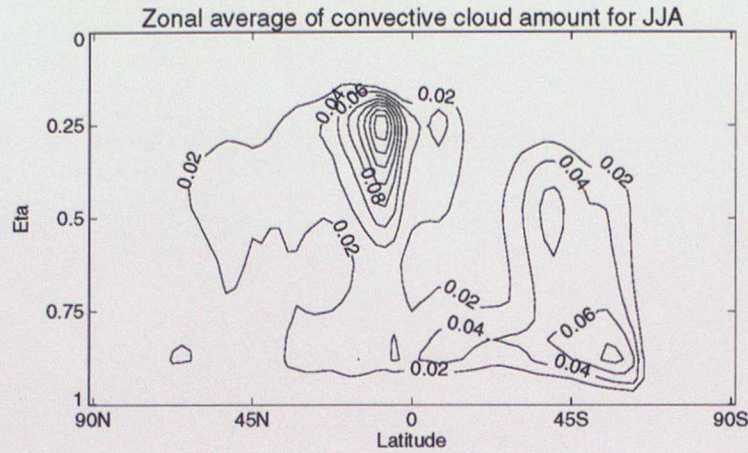


Figure 15: Zonal mean convective cloud amount: ANVIL

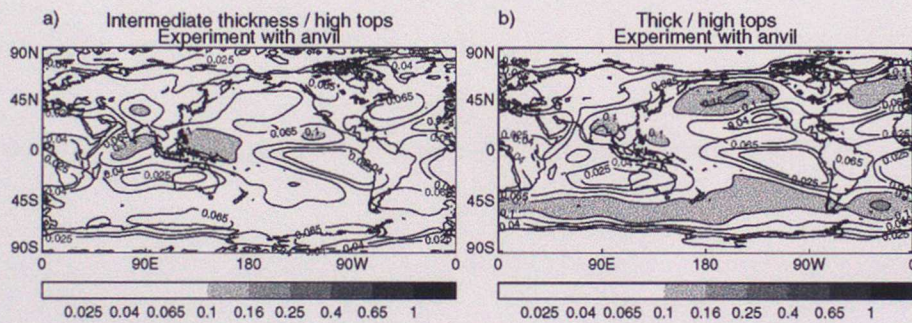


Figure 16: Amounts of medium and high optical thickness clouds with high cloud tops in July 1988: ANVIL

better agreement with ERBE and ISCCP data and more realistic radiative heating rates than the previous representation of convective cloud. It is currently being tested in the development version of the coupled model, in which it is expected to reduce systematic errors by improving the surface and TOA radiation budgets over the tropical oceans. It also reduces a cold bias in the upper tropical troposphere.

The development of a parametrization of mesoscale convective systems is currently underway in the Met. Office (Gray, personal communication). Future work will involve implementing this treatment of the thermodynamic effects of mesoscale anvils and then linking the representation of clouds rather more closely to their internal microphysical and dynamical processes. This should have the benefit of reducing some of the undesirable arbitrariness in the scheme described here and in its predecessor.

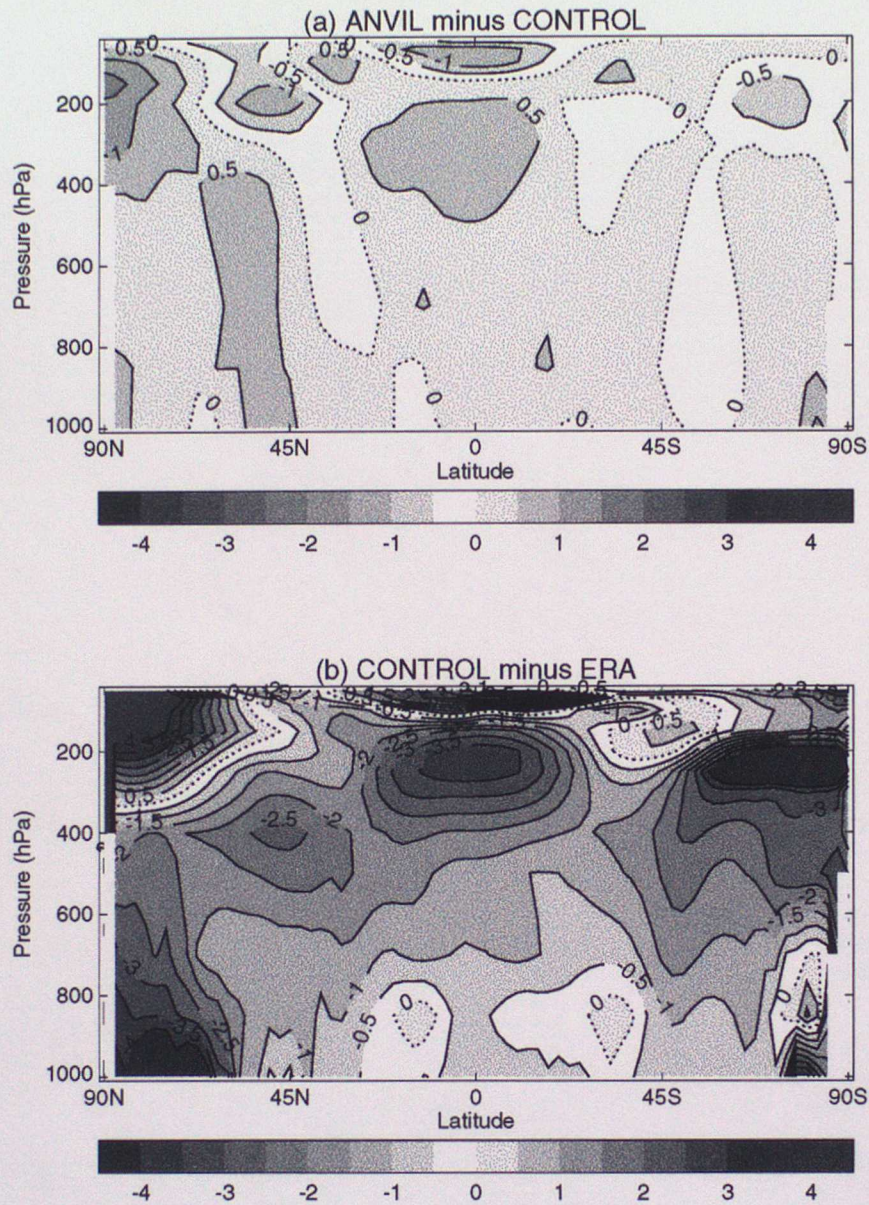


Figure 17: Five year winter average zonal mean temperature difference (K). *Top panel:* ANVIL minus CONT, *Bottom panel:* CONT minus ERA climatology.

9 Acknowledgments

The work benefited from discussions with Mark Webb on the convective cloud optical depths and thanks to him also for providing all plots involving ISCCP data. Thanks also to Tony Slingo for his idea of doing the off-line radiation calculations. I am grateful for Alan Grant's advice on more recent developments to the scheme.

References

- Barkstrom, B. R. (1984). The Earth Radiation Budget Experiment (ERBE). *Bull. Amer. Meteor. Soc.*, **65**, 1170–1185.
- Cusack, S., Edwards, J. M., and Kershaw, R. (1999). A parametrization of the subgrid-scale variability of saturation for use in GCM cloud schemes. *Q. J. R. Meteorol. Soc.*, **submitted**.
- Edwards, J. M. and Slingo, A. (1996). Studies with a flexible new radiation code. Part I. Choosing a configuration for a large-scale model. *Q. J. R. Meteorol. Soc.*, **122**.
- Gregory, D. and Rowntree, P. R. (1990). A mass flux convection scheme with representation of cloud ensemble characteristics and stability-dependent closure. *Mon. Wea. Rev.*, **118**, 1483–1506.
- Martin, G., Smith, R. N. B., Lock, A., Grant, A. L. M., Brown, A., and Bush, M. (1998). The impact of an improved representation of boundary layer mixing on the simulation of clouds in the Unified Model. *Proceedings of the GCSS-WGNE Workshop on Cloud Processes and Cloud Feedbacks in large-scale models, held at ECMWF 9th - 13th November 1998*.
- McClatchey, R., Fenn, R. W., Selby, J. E. A., Volz, F. E., and Garing, J. S. (1972). Optical properties of the atmosphere. (third edition). *U.S. Air Force Cambridge Research Laboratories, Environmental Research Papers*, **411**(AFCRL 72-0497), 110 pp.
- Moncrieff, M., Krueger, S., Gregory, D., Redelsperger, J.-L., and Tao, W.-K. (1997). GEWEX Cloud System Study (GCSS) working group 4: Precipitating convective cloud systems. *Bull. Amer. Meteorol. Soc.*, **78**, 831–845.
- Pope, V. D., Gallani, M. L., Rowntree, P. R., and Stratton, R. A. (1999). The impact of new physical parametrizations in the Hadley Centre climate model - HADAM3. *Clim. Dyn.*, **Submitted**.
- Randall, D. A., Harshvardhan, Dazlich, D. A., and Corsetti, T. G. (1989). Interactions among radiation, convection and large-scale dynamics in a general circulation model. *J. Atmos. Sci.*, **46**, 1943–1970.
- Rossow, W. B. and Schiffer, R. A. (1991). ISCCP cloud data products. *Bull. Am. Meteorol. Soc.*, **72**, 2–20.
- Slingo, A. and Slingo, J. M. (1988). The response of a general circulation model to cloud longwave radiative forcing. *Q. J. R. Meteorol. Soc.*, **114**, 1027–1062.
- Slingo, J. (1987). The development and verification of a cloud prediction scheme for the ECMWF model. *Q. J. R. Meteorol. Soc.*, **113**, 899–927.

- Stratton, R., Pope, V., Gallani, M., and Pamment, J. (1998). HADAM3: the Hadley Centre model - results for AMIP II. *Proceedings of the first WCRP international conference on reanalyses, Silver Spring, Maryland, USA, 27-31 October 1997.*, **WMO/TD 876**.
- Tiedtke, M. (1993). Representation of clouds in large-scale models. *Mon. Wea. Rev.*, **121**, 3040–3061.
- Wilson, D. and Ballard, S. (1999). A microphysically based precipitation scheme for the Meteorological Office Unified Model. *Q. J. R. Meteorol. Soc.*, **in press**.
- Zender, C. S. and Kiehl, J. T. (1997). Sensitivity of climate simulations to radiative effects of tropical anvil structure. *J. Geophys. Res.*, **102**, 23793–23804.